

*Reprinted from*

# APPLIED PHYSICS EXPRESS

## **Room-Temperature Observation of Size Effects in Photoluminescence of $\text{Si}_{0.8}\text{Ge}_{0.2}$ /Si Nanocolumns Prepared by Neutral Beam Etching**

Rii Hirano, Satoru Miyamoto, Masahiro Yonemoto, Seiji Samukawa,  
Kentaro Sawano, Yasuhiro Shiraki, and Kohei M. Itoh

Appl. Phys. Express **5** (2012) 082004

## Room-Temperature Observation of Size Effects in Photoluminescence of Si<sub>0.8</sub>Ge<sub>0.2</sub>/Si Nanocolumns Prepared by Neutral Beam Etching

Rii Hirano<sup>1</sup>, Satoru Miyamoto<sup>1</sup>, Masahiro Yonemoto<sup>2</sup>, Seiji Samukawa<sup>2,3,4</sup>, Kentarou Sawano<sup>5</sup>, Yasuhiro Shiraki<sup>5</sup>, and Kohei M. Itoh<sup>1\*</sup>

<sup>1</sup>School of Fundamental Science and Technology and CREST–JST, Keio University, Yokohama 223-8522, Japan

<sup>2</sup>Institute of Fluid Science, Tohoku University, Sendai 980-8577, Japan

<sup>3</sup>WPI Advanced Institute for Materials Research, Tohoku University, Sendai 980-8577, Japan

<sup>4</sup>Japan Science and Technology Agency, CREST, Chiyoda, Tokyo 102-0075, Japan

<sup>5</sup>Research Center for Silicon Nano-Science, Tokyo City University, Setagaya, Tokyo 158-0082, Japan

Received June 3, 2012; accepted June 26, 2012; published online July 19, 2012

We report the room-temperature observation of clear size effects in photoluminescence of ensembles of SiGe/Si double-quantum-well nanocolumns. A silicon thin layer (~100 nm) containing two 3-nm-thick Si<sub>0.8</sub>Ge<sub>0.2</sub> layers was etched into an ensemble of ~100 nm tall nanocolumns standing vertically on the 200-nm-thick silicon-on-insulator layer. A clear shift of photoluminescence peak positions appearing at around 1.8 eV has been observed with varying average diameter of the nanocolumns between 18 and 24 nm.

© 2012 The Japan Society of Applied Physics

Quantum dots (QDs) are attracting much attention for a wide variety of optoelectronic and quantum information processing applications.<sup>1–3</sup> The characteristic size of QDs must be very small, typically ~20 nm or smaller, to make the quantum confinement effective. Under such a condition, the optical transition energy of QDs changes significantly with the size (quantum size effect).<sup>4</sup> Furthermore, higher QD density (number of QDs per unit area or volume), size uniformity, and ordering are very often demanded for optoelectronic applications. Thus far, ensembles of QDs formed by self-assembly are the most promising towards highly efficient optical devices.<sup>5,6</sup> In order to improve the size dispersion and density that cannot be controlled precisely by the self-assembly method, efforts have also been made towards forced assembly of QDs and/or top-down formation of QDs by lithography and etching.<sup>7–9</sup> The top-down approaches are preferred from the production point of view due to its cost effectiveness. However, in general, QDs made by the top-down approaches exhibit poor electronic and optical characteristics due to surface defects incorporated during etching processes.<sup>10–12</sup> Therefore, the development of QD formation technologies leading to efficient light emission and the demonstration of quantum effects are strongly demanded.

The present paper reports the observation of bright emission and clear size effects arising from ensembles of SiGe-based QDs formed by neutral-beam etching of Si<sub>0.8</sub>Ge<sub>0.2</sub>/Si double-quantum-well layers.

The Si<sub>0.8</sub>Ge<sub>0.2</sub>/Si double-quantum-well structure has been grown by gas source molecular beam epitaxy as described in refs. 13 and 14. A silicon-on-insulator (SOI) wafer with the top silicon layer having 200 nm thickness was employed to suppress the escape of electron–hole pairs to the substrate. First, a 50 nm Si buffer layer was grown followed by the growth of a 3-nm-thick Si<sub>0.8</sub>Ge<sub>0.2</sub> layer, a 30 nm Si layer, a 3 nm Si<sub>0.8</sub>Ge<sub>0.2</sub> layer, and a 30 nm cap Si layer. Such a quantum well structure leads to bright emission of light by trapping holes in Si<sub>0.8</sub>Ge<sub>0.2</sub> layers and electrons in the Si layers (Type II alignment).<sup>15</sup> The present Si<sub>0.8</sub>Ge<sub>0.2</sub>/Si double-quantum-well structures before etching yielded low-temperature PL spectra that were essentially the same as

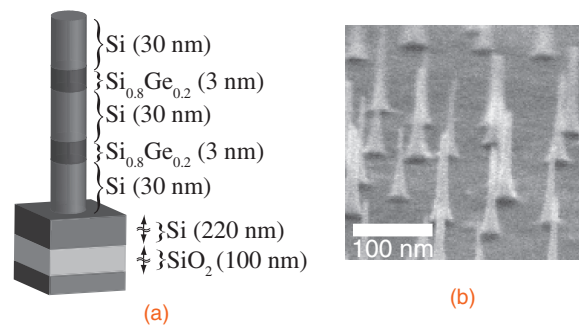
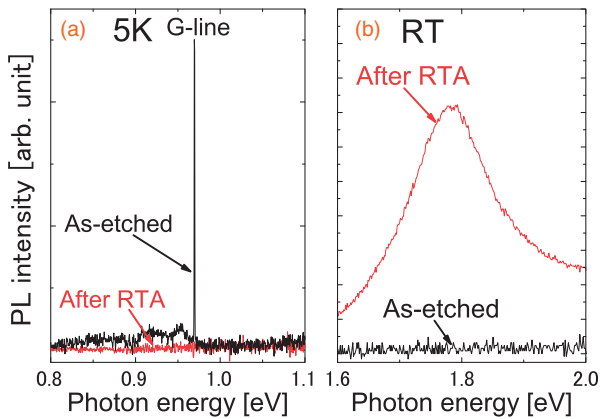


Fig. 1. (a) Schematic of Si<sub>0.8</sub>Ge<sub>0.2</sub>/Si nanocolumns formed on a SOI wafer and (b) SEM image of Si<sub>0.8</sub>Ge<sub>0.2</sub>/Si nanocolumns.

the ones reported in refs. 13 and 14. Then, etching of the double-quantum-well structure using a neutral beam led to the formation of ensembles of nanocolumns having the geometry shown in Fig. 1(a). The details of the neutral-beam etching using protein-derived masking methods are given in refs. 16 and 17. In short, recombinant ferritin particles having artificially hydrated iron oxide (5Fe<sub>2</sub>O<sub>3</sub>·9H<sub>2</sub>O) cores were dropped onto the wafer and dispersed uniformly by centrifuging at 10,000 rpm. Less than one monolayer of ferritin molecules were absorbed on the wafer by this process. A UV/ozone treatment was performed to remove the ferritin protein shells, leaving the iron cores that were to be used as masks against etching. Then, the sample was etched down for a depth of ~100 nm using neutral chlorine beams and immersed in 5 M hydrochloric solution for 10 min to remove the residual iron masks. A scanning electron microscopy (SEM) image of Si<sub>0.8</sub>Ge<sub>0.2</sub>/Si nanocolumns is shown in Fig. 1(b). While better control of the nanocolumn position and density was possible, the present study proceeded with the disorder as shown in Fig. 1(b) because our primary interest was the observation of photoluminescence (PL) with quantum size effects from the Si<sub>0.8</sub>Ge<sub>0.2</sub>/Si nanocolumns prepared by our top-down approach.

Macroscopic PL and microscopic PL spectroscopies were performed at temperatures of 5 K and room temperature, respectively. In the macroscopic PL, the 351 and 364 nm lines of an Ar ion laser with the spot diameter of ~2 mm were used as excitation sources. The emission was analyzed

\*E-mail address: kitoh@appi.keio.ac.jp

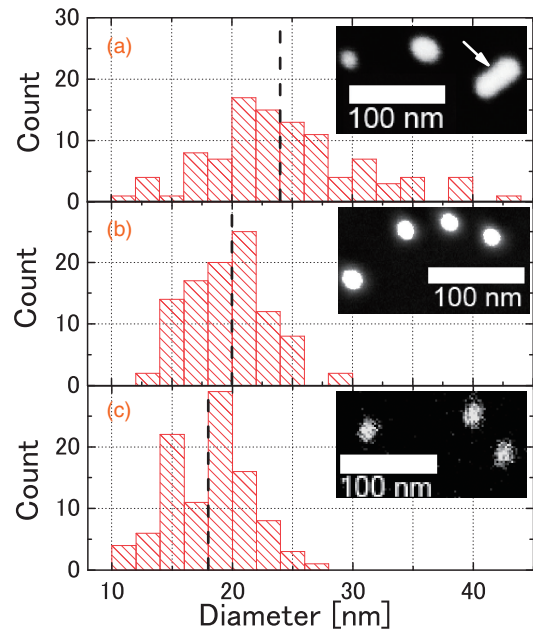


**Fig. 2.** PL spectra of  $\text{Si}_{0.8}\text{Ge}_{0.2}/\text{Si}$  nanocolumns as-etched and after RTA in the (a) infrared region at 5 K and (b) visible region at room temperature.

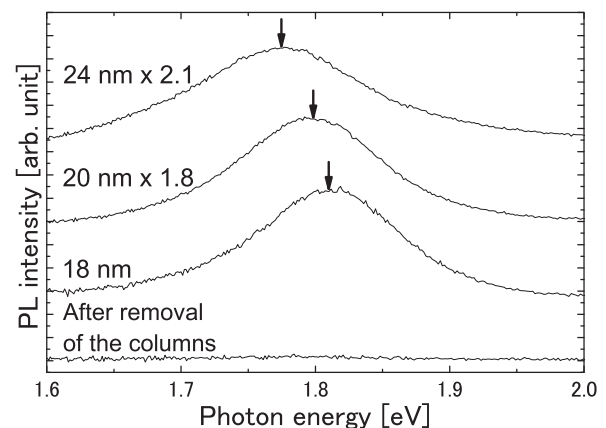
using a Fourier transform infrared spectrometer equipped with an InGaAs detector. The sample was cooled by a continuous He flow cryostat. In the microscopic PL spectroscopy, the 514.5 nm line of an Ar ion laser was focused on the samples to achieve the spot diameter of  $\sim 2\ \mu\text{m}$ . The emission was spectrally dispersed by a single grating with a spectral resolution of about 3 meV and detected with a charge-coupled device camera. Averaging of ten spectra measured at randomly chosen surface points was conducted to obtain a representing spectrum of each sample.

Figure 2(a) shows a PL spectrum of as-etched  $\text{Si}_{0.8}\text{Ge}_{0.2}/\text{Si}$  nanocolumns in the macroscopic geometry. Well-known 0.97 eV luminescence (G-line) due to bistable carbon-interstitial-carbon-substitutional pairs<sup>18)</sup> and their phonon replica appear. Carbon impurities might have been introduced unintentionally during the MBE growth. We found that these defects could be annihilated easily by rapid thermal annealing (RTA) at 900 °C for 15 s [Fig. 2(a)]. In Fig. 2(b), although we could not observe any spectra from as-etched  $\text{Si}_{0.8}\text{Ge}_{0.2}/\text{Si}$  nanocolumns at room temperature, a bright PL peak appeared at around 1.8 eV after RTA.

In order to show that the broad PL peak at  $\sim 1.8\ \text{eV}$  arises from the nanocolumns, the size dependence of the PL emission wavelength is investigated. More specifically, the size of the nanocolumns was reduced by natural oxidation in air at room temperature for days followed by the removal of the oxide layer by dipping the entire structure into 5% hydrofluoric (HF) solution for 30–60 s. After PL measurements of this set of nanocolumn ensemble, the size of the nanocolumns was reduced further by annealing in air at 780 °C for 6 min to form oxide layers around the nanocolumns followed by HF dipping. We confirmed the reduction of  $\text{Si}_{0.8}\text{Ge}_{0.2}/\text{Si}$  nanocolumn diameters by SEM observation in each sample. In Figs. 3(a)–3(c), the histograms of the  $\text{Si}_{0.8}\text{Ge}_{0.2}/\text{Si}$  nanocolumn diameters are constructed by measuring the diameters of 100 nanocolumns in corresponding SEM images shown in the insets. As a result, nanocolumns are found to have the average diameters of 24, 20, and 18 nm. Not only circular but also large elliptical nanocolumns are seen as indicated by a white arrow in Fig. 3(a). Such elliptical nanocolumns are composed of two nanocolumns situated close to one another and are formed when two iron core masks existed close to one another during etching.



**Fig. 3.** Histograms of  $\text{Si}_{0.8}\text{Ge}_{0.2}/\text{Si}$  nanocolumns (a) immediately after neutral beam etching, (b) after removal of the naturally formed surface oxide by HF, and (c) after single cycle of oxidation annealing and HF as described in the text. Insets show top-view images of the corresponding nanocolumns recorded by SEM. The diameters of 100 nanocolumns (white circles in the insets) are measured to construct a corresponding histogram. Dashed lines indicate the average diameter of nanocolumns. A white arrow in (a) indicates the presence of an elliptical shaped nanocolumn pair as described in the text.



**Fig. 4.** Room temperature PL spectra of ensembles of 24-, 20-, and 18-nm-average-diameter  $\text{Si}_{0.8}\text{Ge}_{0.2}/\text{Si}$  nanocolumns shown in Figs. 3(a)–3(c), respectively. The intensities of the 24- and 20-nm-average-diameter nanocolumns are adjusted by 2.1 and 1.8 times of the original intensities, respectively, to highlight the shift in the emission energy. The arrows indicate the peak positions. The bottom spectrum shows the disappearance of the characteristic emission after the complete removal of the nanocolumns by further etching.

The HF dipping tends to separate such nanocolumn pairs into isolated single nanocolumns. As a result, the standard deviation of the diameters was reduced from 6 to 3 nm by HF dipping. Figure 4 shows the PL spectra recorded at room temperature with the ensembles of nanocolumns shown in Figs. 3(a)–3(c), and after a third cycle of oxidation and dipping, which removed the  $\text{Si}_{0.8}\text{Ge}_{0.2}/\text{Si}$  nanocolumns

completely. The disappearance of PL at  $\sim 1.8$  eV after the removal of the  $\text{Si}_{0.8}\text{Ge}_{0.2}/\text{Si}$  nanocolumns suggests that the  $\sim 1.8$  eV PL arises from the  $\text{Si}_{0.8}\text{Ge}_{0.2}/\text{Si}$  nanocolumns. Furthermore, the  $\sim 1.8$  eV PL peak position exhibits a blue shift as the average diameter is reduced from 24 to 18 nm as expected from the quantum size effect. The shifts of the peak position with respect to the 24-nm-average-diameter nanocolumns are 25 meV for the 20-nm-average-diameter columns and 32 meV for the 18-nm-average-diameter nanocolumns. The full widths at the half maximum (FWHMs) are also reduced from that of the 24-nm-average-diameter sample by 30% for 20 nm and by 36% for the 18-nm-average-diameter nanocolumns, reflecting the reduction of the size dispersion in the histograms shown in Figs. 3(a)–3(c). The increase of the PL intensity with the reduction in the average diameter indicates the increase of the quantum efficiency in the smaller quantum dots.

While some authors claim the origin of similar blue shifts from silicon nanostructures to be the quantum size effect,<sup>19)</sup> others attribute them to emission from silicon-oxide-related defects.<sup>20,21)</sup> Valenta *et al.* have reported bright emission of light from single Si nanostructures fabricated by lithography and reactive ion etching.<sup>22)</sup> However, the emission was observed only after surface thermal oxidation. In our case, the emission was observed even after the removal of the surface oxide by HF.

One may claim that the blue shift of the PL can arise also from the relaxation of the strain in the  $\text{Si}_{0.8}\text{Ge}_{0.2}$  layers, which can change the hole trapping energy of the  $\text{Si}_{0.8}\text{Ge}_{0.2}$  QD in the nanocolumns. Indeed, in the case of  $\text{Si}_{0.8}\text{Ge}_{0.2}$  layers formed on Si, the hole trapping energy in the fully relaxed case is  $\sim 30$  meV less than that in the fully strained case.<sup>23)</sup> Therefore, the blue shift of  $\sim 30$  meV is expected when the strain in  $\text{Si}_{0.8}\text{Ge}_{0.2}$  QDs is removed completely. This  $\sim 30$  meV is comparable to the blue shift of  $\sim 32$  meV observed between 24- and 18-nm-average-diameter nanocolumns. However, considering the thinness (3 nm) of the  $\text{Si}_{0.8}\text{Ge}_{0.2}$  layers in our case, it is hard to believe that the thin  $\text{Si}_{0.8}\text{Ge}_{0.2}$  QDs sandwiched by the thick Si stressors can change from fully strained to fully relaxed states between the average diameters of 24 and 18 nm. Therefore, although there may be some contribution of the strain relaxation, we believe that the blue shift is caused predominantly by the quantum size effect. It should also be pointed out that, if  $\text{SiO}_2$  had surrounded the side wall of each nanocolumn, the resulting strain would have led to the red shift in PL.

In summary,  $\text{Si}_{0.8}\text{Ge}_{0.2}/\text{Si}$  nanocolumns have been fabricated successfully by the combination of molecular beam epitaxy and neutral beam etching. After rapid thermal

annealing, the photoluminescence of  $\sim 1.8$  eV was observed at room temperature. The control of the average diameter of  $\text{Si}_{0.8}\text{Ge}_{0.2}/\text{Si}$  nanocolumns between 24 and 18 nm has been achieved by repetition of the thermal oxidation and HF dipping cycle. The blue shift in PL, predominantly due to quantum size effect, has been observed as the average diameter of the nanocolumns is reduced.

**Acknowledgments** The work at Keio was supported in part by a Grant-in-Aid for Scientific Research and the Project for Developing Innovation Systems by the Ministry of Education, Culture, Sports, Science and Technology (MEXT). RI was supported by a Grant-in-Aid for the Global Center of Excellence for High-Level Global Cooperation for Leading-Edge Platform on Access Spaces from MEXT. The work at Tokyo City University was supported by the project for strategic advancement of research infrastructure for private universities 2009–2013, by a Grant-in-Aid for Scientific Research from MEXT and by the Industrial Technology Research Grant Program from NEDO.

- 1) Y. Arakawa and H. Sakaki: *Appl. Phys. Lett.* **40** (1982) 939.
- 2) E. Biolatti, R. C. Iotti, P. Zanardi, and F. Rossi: *Phys. Rev. Lett.* **85** (2000) 5647.
- 3) M. Ohtsu, K. Kobayashi, T. Kawazoe, S. Sangu, and T. Yatsui: *IEEE J. Sel. Top. Quantum Electron.* **8** (2002) 839.
- 4) T.-Y. Kim, N.-M. Park, K.-H. Kim, G. Y. Sung, Y.-W. Ok, T.-Y. Seong, and C.-J. Choi: *Appl. Phys. Lett.* **85** (2004) 5355.
- 5) S. Fukatsu, H. Sunamura, Y. Shiraki, and S. Komiyama: *Appl. Phys. Lett.* **71** (1997) 258.
- 6) M. Elkurdi, P. Boucaud, S. Sauvage, O. Kermarrec, Y. Campidelli, D. Bensahel, G. Saint-Girons, and I. Sagnes: *Appl. Phys. Lett.* **80** (2002) 509.
- 7) S.-H. Choi, J. N. Kim, H. Y. Kim, Y.-K. Hong, J.-Y. Koo, J. H. Seok, and J. Y. Kim: *Appl. Phys. Lett.* **80** (2002) 2520.
- 8) P. B. Fischer, K. Dai, E. Chen, and S. Y. Chou: *J. Vac. Sci. Technol. B* **11** (1993) 2524.
- 9) G.-R. Lin, C.-J. Lin, H.-C. Kuo, H.-S. Lin, and C.-C. Kao: *Appl. Phys. Lett.* **90** (2007) 143102.
- 10) H. Ootera, T. Oomori, M. Tsuda, and K. Namba: *Jpn. J. Appl. Phys.* **33** (1994) 4276.
- 11) T. Nozawa, T. Kinoshita, T. Nishizuka, A. Narai, T. Inoue, and A. Nakaue: *Jpn. J. Appl. Phys.* **34** (1995) 2107.
- 12) T. Kinoshita, M. Hane, and J. P. McVittie: *J. Vac. Sci. Technol. B* **14** (1996) 560.
- 13) S. Fukatsu, N. Usami, Y. Kato, H. Sunamura, Y. Shiraki, H. Oku, T. Ohnishi, Y. Ohmori, and K. Okumura: *J. Cryst. Growth* **136** (1994) 315.
- 14) Y. Shiraki, H. Sunamura, N. Usami, and S. Fukatsu: *Appl. Surf. Sci.* **102** (1996) 263.
- 15) T. Baier, U. Mantz, K. Thonke, R. Sauer, F. Schäffler, and H.-J. Herzog: *Phys. Rev. B* **50** (1994) 15191.
- 16) T. Kubota, T. Baba, S. Samukawa, H. Kawashima, Y. Uraoka, T. Fuyuki, and I. Yamashita: *Appl. Phys. Lett.* **84** (2004) 1555.
- 17) S. Samukawa: *Jpn. J. Appl. Phys.* **45** (2006) 2395.
- 18) L. W. Song, X. D. Zhan, B. W. Benson, and G. D. Watkins: *Phys. Rev. B* **42** (1990) 5765.
- 19) M. V. Wolkin, J. Jorne, P. M. Fauchet, G. Allan, and C. Delerue: *Phys. Rev. Lett.* **82** (1999) 197.
- 20) G. Qin and G. G. Qin: *J. Appl. Phys.* **82** (1997) 2572.
- 21) G. G. Qin and Y. J. Li: *Phys. Rev. B* **68** (2003) 085309.
- 22) J. Valenta, R. Juhász, and J. Linnros: *Appl. Phys. Lett.* **80** (2002) 1070.
- 23) J. Liu, A. Zaslavsky, B. R. Perkins, C. Aydin, and L. B. Freund: *Phys. Rev. B* **66** (2002) 161304.